J Wood Sci (2016) 62:42–51
DOI 10.1007/s10086-015-1520-9

ORIGINAL ARTICLE

Detection of decay damage in iron-wood living trees by nondestructive techniques

Cheng-Jung Lin[1] · Yue-Hsing Huang[2] · Gwo-Shyong Huang[1] · Meng-Ling Wu[3]

Received: 9 July 2015 / Accepted: 27 September 2015 / Published online: 23 October 2015

Abstract The purpose of this study was to investigate the standard values of living, undamaged iron-wood (*Casuarina equisetifolia*) trees by different nondestructive techniques. This study also detects the transversal stress wave velocity (V) and tomogram, and resolves corresponding V maps of the trees with and without decay damage. First, a visual tree inspection form with seven categories of tree defects is proposed for tree hazard assessment. The range of demarcation between decay-damaged and sound wood occurred at an approximate V of 1461–1636 m/s by transversal stress wave velocity tomography. Different nondestructive evaluation parameters can serve as an index for diagnosing standard values (with or without decay). A positive significant relationship was found between the diameter and transversal minimum V of 2D in undamaged trees. Moreover, the product diameter × frequency of evaluated value by lateral impact vibration method tended to increase with increasing minimum V of 2D using tomography in undamaged and decay-damaged trees. Decay damage in iron-wood living trees could be inspected and detected by lateral impact vibration method and transversal stress wave velocity tomography for the general location and area of wood deterioration.

✉ Cheng-Jung Lin
d88625002@yahoo.com.tw

[1] Forest Utilization Division, Taiwan Forestry Research Institute, 53 Nanhai Rd., Taipei 10066, Taiwan

[2] Taiwan Forestry Research Institute, 53 Nanhai Rd., Taipei 10066, Taiwan

[3] Forest Protection Division, Taiwan Forestry Research Institute, 53 Nanhai Rd., Taipei 10066, Taiwan

Keywords Stress wave velocity · Tree risk assessment · Visual tree inspection · Nondestructive technique · Tomogram

Introduction

The iron-wood (*Casuarina equisetifolia*) tree is a common landscape tree near seacoast in Taiwan. This type of tree often plants along both sides of the road for windbreak tree or protect forest. These trees growing on the roadside suffer from man-made and natural decay damage (Fig. 1), and often fall without warning. This could lead to risk of human casualties or result in property loss.

Concerns about public safety and urban tree conservation strongly support the development and application of rapid, precise, and cost efficient diagnostic techniques to detect decay and other types of structural defects in trees [1]. Standing trees must be evaluated to maintain in situ structural safety for tree risk assessment. Various nondestructive techniques (NDT) have been applied to detect decay and deterioration in trees to identify hazardous trees. NDT is the science of identifying the physical and mechanical properties of a piece of material without altering its end-use capabilities and then using this information to make decisions regarding appropriate applications [2]. Visual tree assessment, a systematic method of tree assessment using biological and biomechanical indicators to evaluate overall vitality and structural integrity of a tree, includes visual inspection of the tree to look for external evidence of internal defects, instrumental measurements of internal defects and evaluation of the residual strength of the wood [3]. Arboriculturists consider visual tree assessment (i.e., structural defects) an essential practice. This kind of assessment serves as the starting point for

Fig. 1 Decay damage of iron-wood (*Casuarina equisetifolia*) street tree

evaluating tree defects and providing basic information about tree growth performance and stability. Tree breakage depends on many features of the tree, including its height, width of crown, crown architecture, crown density in the branching and leaves, form, condition, physical wood properties, and species [4].

Stress wave or ultrasonic velocity evaluation measurements of wood have proven to be effective parameters for detecting and estimating deterioration in tree trunk and wood structures [2, 5]. NDT have been developed for tomographic investigation [6]. Stress wave or ultrasonic tomographic measurements in wood have been found to be effective in detecting and estimating decay in tree trunks [1, 7–15]. Stress wave or ultrasonic tomography has been proven to be the most effective technique for detecting internal decay, locating the position of defects, and estimating their size, shape and characteristics. In addition, because the location of decay is more important in terms of strength loss than just the size of the area of decay, stress wave or ultrasonic tomography allows specialist to determine relative strength loss [16].

A fractometer is a device that breaks the radial increment core along the direction of the fiber to measure the fracture strength [17]. Many diagnostic devices such as resistographs, stress wave or ultrasonic detectors, electrical conductivity meters and fractometers are available for detecting internal decay and other defects in living trees [18]. These NDT can be used in combination to achieve better accuracy in determining the location and extent of wood deterioration.

No detailed reports have been published about detecting wood decay damage in iron-wood (*Casuarina equisetifolia*) living trees by different nondestructive techniques. Therefore, the first objective of this study was to detect the evaluation parameters of living, undamaged (without decay) iron-wood trees by stress wave velocity tomography, lateral impact vibration, fractometer, and density profile techniques. We also generated tables of standard values (references) to aid in the use of these methods in wood deterioration surveys. A secondary objective was carried out to investigate transversal stress wave velocity tomogram (VT) and resolve corresponding stress wave velocity (V) maps of iron-wood trees with decay damage to understand the degree and extent of trunk deterioration for tree risk assessment.

Materials and methods

First, the experiment was carried out in situ on 34 sound iron-wood trees in Miaoli county (18 sampled trees) and Tanyuan city (16 sampled trees), Taiwan. These trees were inspected in December, 2014, when the trees were about 30–50 years old with average diameters at breast height (DBHs) of 39.2 cm. Multiple stress wave measurements (Fakopp enterprise, Agfalva, Hungary) were carried out at eight equidistant points (eight probes) along the circumference of the trunks. All sensors were located in the trees at about 130 cm above ground and the transducer was connected at an angle of 90° to the trunk axis to detect the propagated travel time and stress wave velocities. The transmitter probe was first positioned at point 1 with stress wave pulses acquired by the receiver probe at the other seven points. Hammer tapping was done from points 1 to 8, respectively. Measurements were repeated with the transmitter probe positioned at each point, thus giving 28 [for a complete round trip: 7 receiving probes × 8 transmitter probes ÷ 2 (the same path was measured twice)] independent propagation time measurements for each investigated section. A complete data matrix was obtained through this measurement process at each test location.

The circumference of each cross section and the distances between sensors were measured using a tape measure. These measurements served as inputs for the system

software to map the approximate geometric form of the cross sections. First, upon completing stress wave velocity measurements, a tomogram was constructed for each cross section using the ArborSonic software. Second, due to differences in species and paths, a two-dimensional (2D) image was obtained using the above software based on original stress wave transmission times (no adjusted and regularized times) to help better understand the experimental values in this study. To quantitatively assess the tomograms, all corresponding stress wave velocities were further calculated at each pixel of the tomogram were further calculated by visualizing and converting the tomograms to yield stress wave velocity maps of the cross sections (e.g., Figs. 2, 3).

After the stress wave velocity information of each cross section provided by the tomograms was tabulated, the resonant frequencies were measured using a portable lateral impact vibration meter (Ponta, World Enterprise, Japan) to diagnose the wood quality inside a standing tree. The product $D \times F$ (m Hz) of the resonance frequency F of the vibration or the sound of an impacted tree trunk and the trunk diameter D serve as the diagnosis index.

Finally, 5-mm diameter cores were cut from the trunk using an increment borer. A fractometer was used to evaluate the crushing strength of core samples (in green state) in the bark to the pith direction at an interval of 6 mm. Finally, a core specimen was mounted and processed into slices (wideness $\times$ thickness $= 17 \times 2.0$ mm) for X-ray densitometric scanning. The conditioned slices (air-dried) were subjected to a direct-reading X-ray densitometer (QTRS-01X Tree Ring Analyzer, Quintek Measurement Systems (QMS), Knoxville, TN, USA) to determine the tree ring (wood) density profile. Table 1 summarizes these nondestructive evaluation methods used for tree assessment in this experiment.

The experiment was also carried out in situ on 15 different decay-damaged iron-wood street trees (trees planted along both sides of the road) in Miaoli county (ten sampled trees) and Tanyuan city (five sampled trees), Taiwan. These trees were investigated in December, 2014, when the trees were about 30–50 years old with DBHs of 42.2 cm. Tree trunk deterioration was detected by stress wave velocity tomography (using the same method described above). After the stress wave velocity tomography information (2D image) of each cross section provided by the tomogram was tabulated, the sampling core method was conducted using an increment corer to understand the wood deterioration (with or without decay damage) by the visual method. Finally, the resonant frequencies were measured using a portable lateral impact vibration meter to diagnose the living tree and the product $D \times F$ (m Hz) serve as the diagnosis index (as described above).

Results

Seven categories of tree defects and appearance were inspected by the visual tree inspection form (Table 2). The seven main defects were decayed wood, cracks, root problems, weak branch unions, cankers, poor tree architecture (trunk and branch), and dead trees, tops, or branches. First, the iron-wood trees were inspected visually, focusing on different decay-damaged trees.

The evaluated parameters of different nondestructive techniques, including the average lateral impact vibration performance, green crushing strength, and air-dried wood density were 358.0 m Hz, 34.4 MPa, and 875.8 kg/m^3, respectively (Table 3). The lateral impact vibration performance, green crushing strength, and air-dried wood density of a normal undamaged tree stem serves as the index of diagnosis or standard reference value.

The average minimum and maximum stress wave velocity (V_{min} and V_{max}) values were 1636 and 2539 m/s for the 24 undamaged iron-wood trees, respectively (Table 4). The mean stress wave velocity (V_{mean}) of the tomogram was 2087 m/s. The V_{min} and V_{max} values were 1404 and 2570 m/s for the 15 decay-damaged iron-wood trees, respectively (Table 5). The V_{mean} of the tomogram was 1987 m/s. Average V_{min} value of the trunks in decay-damaged trees (Table 5) was clearly lower than that of the undamaged trees (Table 4). The V_{min} value (1636 m/s) can be considered as the threshold values of diagnosis by stress wave velocity tomogram.

The VT and corresponding V value maps were examined for the 34 undamaged and 15 decay-damaged iron-wood trees (Figs. 2, 3). The sampling core method was conducted using an increment corer to understand the wood deterioration. None of the tomograms of the undamaged iron-wood trees displayed a distinct pattern of high and low V in the cross section of the stem (Fig. 2). However, all tomograms of the decay-damaged iron-wood trees displayed a distinct pattern of high V (undamaged wood area) and low V (decay-damaged wood area) at the stem perimeter or center (Fig. 3). The standard deviation values of V_{min} in decayed damaged trees (Table 5) were clearly higher than that of undamaged trees (Table 4).

The relationships between transversal stress wave velocities (V_{min}, V_{max}, and V_{mean}) with the 2D diameters of undamaged iron-wood trees are shown in Fig. 4. The V_{min}, V_{max}, and V_{mean} values generally increased with increasing diameter values. When expressed as the linear regression relationships, the determined coefficients (R^2) were 0.65–0.75. Statistical analysis showed that the relationships between stress wave velocity and diameter values were significant at 0.01 levels. This result shows that these V_{min} values (about 1300–2000 m/s) tended to increase with

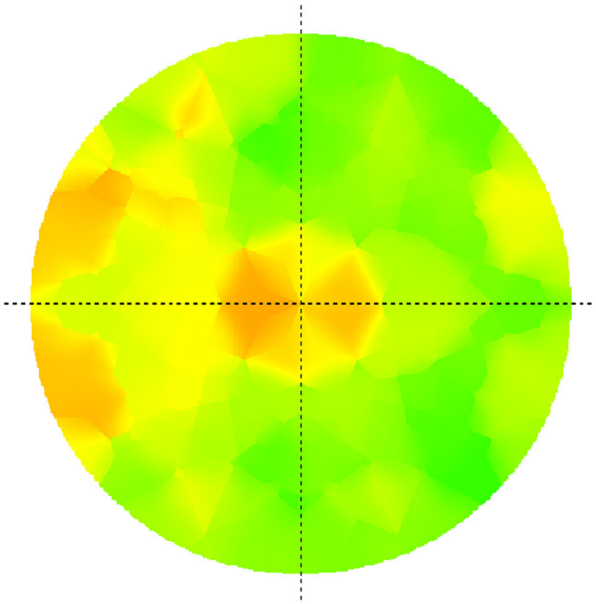

					2254	2271	2262	2354	2400	2373					
			2267	2231	2243	2283	2316	2389	2388	2353	2374	2401			
		2304	2301	2195	2228	2341	2415	2399	2367	2315	2344	2405	2417		
	2206	2245	2252	2237	2284	2412	2444	2402	2368	2315	2333	2377	2390	2297	
	2134	2125	2180	2207	2291	2358	2383	2371	2349	2330	2352	2354	2288	2231	
2125	2120	2155	2193	2179	2253	2336	2314	2321	2345	2349	2383	2370	2299	2225	2230
2138	2146	2211	2232	2207	2213	2191	2182	2214	2234	2302	2324	2362	2355	2255	2263
2165	2236	2249	2223	2207	2180	2092	2124	2167	2137	2253	2302	2314	2373	2382	2342
2165	2244	2246	2217	2202	2170	2083	2105	2143	2121	2229	2284	2296	2372	2406	2365
2130	2141	2211	2229	2200	2195	2153	2152	2183	2191	2269	2294	2356	2375	2308	2308
2116	2116	2169	2223	2209	2245	2297	2268	2274	2307	2325	2393	2419	2369	2295	2291
	2125	2148	2232	2245	2290	2320	2339	2333	2323	2351	2420	2442	2376	2315	
	2202	2278	2290	2280	2306	2376	2408	2374	2362	2358	2412	2459	2451	2356	
		2338	2344	2267	2275	2362	2410	2380	2346	2307	2361	2452	2476		
			2323	2289	2289	2345	2385	2381	2353	2325	2361	2388			
					2326	2356	2362	2374	2376	2364					

Fig. 2 Stress wave velocity tomogram and the corresponding stress wave velocity map grids (3 × 3 cm) of an undamaged tree (no. 7, velocity range, 1839–2558 m/s)

increasing diameter (about 20–60 cm). Different diameter classes of tree affected the V_{min}, V_{max}, V_{mean} of tomogram. The V_{min} value can be considered as the threshold value of diagnosis by stress wave velocity tomography, and the V value was affected by diameter. Therefore, the V threshold value should be adjusted with the 2D diameter values.

The relationship between the diameter × frequency ($D \times F$ value, lateral impact vibration performance, m Hz) and the stress wave velocity (V_{min}, V_{max}, and V_{mean}) values (m/s) of tomogram in undamaged and damaged trunk cross section is presented in Fig. 5. The $D \times F$ values generally increased with increasing stress wave velocity (V_{min}, V_{max},

and V_{mean}) values. When expressed as the linear regression relationships, the determined coefficients (R^2) were 0.25–0.43. Statistical analysis showed the relationships between $D \times F$ and stress wave velocity (V_{min}, V_{max}, and V_{mean}) values were significant at 0.01 levels. The result displayed that the $D \times F$ value of lateral impact vibration performance in undamaged or damaged living trees serves as the index of diagnosis for general soundness or preliminary decay status. Moreover, the stress wave velocity tomogram and the corresponding stress wave velocity maps of decay-damaged and undamaged iron-wood tree can detect the general location and area of wood deterioration.

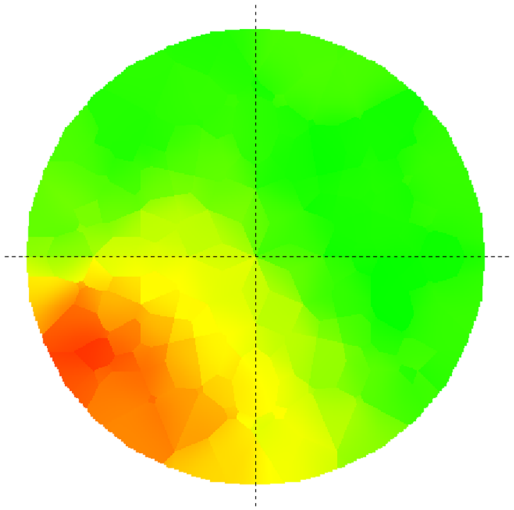

			1999	1992	1915	1905			
		1996	1972	1973	1978	1937	1965	2029	
	1948	1998	1929	1924	2009	2060	2048	2009	
1826	1858	1854	1772	1830	1981	2044	2024	1996	1963
1792	1722	1600	1576	1662	1902	2001	2039	2033	2010
1429	1343	1393	1437	1503	1699	1917	2044	2065	2007
1066	1022	1163	1338	1443	1582	1778	1977	2014	1962
	953	1042	1221	1371	1489	1677	1853	1949	
		1078	1143	1302	1454	1564	1746	1901	
			1220	1322	1428	1519			

Fig. 3 Stress wave velocity tomogram and the corresponding stress wave velocity map grids (3 × 3 cm) of a damaged tree (no. 8, velocity range, 731–2102 m/s)

Discussion

The average transversal stress wave velocity (V), lateral impact vibration performance ($D \times F$), green crushing strength (C), and air-dried wood density (D) of a normal undamaged tree stem serves as the diagnosis index or standard reference value. We present a table of standard values for the future use of these device or methods for testing iron-wood trees. The $D \times F$, C, and D values of three tree species are compared and displayed in Table 3 for comparison [19, 20]. The average V_{min} values of iron-wood, Norfolk island pine, and hoop pine trees are 1636, 1129–1296, and 1154–1164 m/s, respectively. If detected values of nondestructive evaluation are lower than these reference values, the wood quality of the trunk show brings up questions which could require further investigation.

In this study, lower transversal stress wave velocities (map grids) were observed inside of the decay-damaged trees. Severe wood decay defects in have been reported when the stress wave velocity is reduced to 70 % of the characteristic values of sound wood [21]. In this study, the V_{mean} value in the undamaged trees was 2087 m/s with the threshold at 1461 m/s (2087 × 0.7 m/s). Moreover, the average V_{min} value of the tomogram in the undamaged trees was 1636 m/s. Therefore, the range of V_{min} values (1461–1636 m/s) can be considered as the threshold values for diagnosis by stress wave velocity tomogram. Furthermore, the range of demarcation between decay-damaged and undamaged wood occurred at an approximate transversal stress wave velocity of 1461–1636 m/s. The reduction in stress wave velocity is indicative of serious damage, the location and extent of which can be seen in the

Table 1 Assessment of standard values (reference) in sound trees by different nondestructive techniques for tree hazard assessment

Item	Methods	Evaluated parameter
1	Visual tree inspection	Tree inspection form
2	Stress wave device 2D tomogram	Transversal stress wave velocity (m/s)
3	Lateral impact vibration	Diameter × frequency (m Hz)
4	Increment borer	Visual observation of core
5	Fractometer	Crushing strength (green, MPa)
6	X-ray wood density profile	Density (air dried, g/cm^3)

Table 2 Visual tree inspection form with seven categories of tree defects

Defects	Items ■ detected □ undetected
1. Decayed wood	□Decay or rotten □fungi, fungal fruiting body □cavity □hollows, hole □inrolled cracks □ever-expanding column of decay □bulge and swellings □others; e.g., wound, wood discoloration, canker
2. Cracks	□Splitting of weak branch unions □by pruning; e.g., flush-cut pruning, topping □Wind (damage, sap flow, or bleeding)
	□Vertical crack □shear crack □inrolled crack □ribbed crack
	□Horizontal crack
	□Seam
3. Root problems	□Damage □dead □ lost □ crack □decay □lean □fungal fruiting body □root breakage □stem girdling root □others; e.g., disease, disorder, ants, etc.
	□Critical root radius was disturbed, damaged or restricted leading to reduced anchoring ability of roots
	□Crown decline
	□Lean □soil mounding □soil cracking □root lifting
4. Weak branch unions	□Co-dominant stems or branches □epicormic branch □included bark □others; e.g., topping, injured, pruned, crack, or declining branches
5. Cankers	□Canker □fungi □ insect (e.g., termite) □microorganism □mechanical damage □other; e.g., lightning
6. Poor tree architecture (trunk and branch)	□Leaning □tension or buckle symptom □epicormic branch, harp tree □unbalance crown □others; e.g., bends, twists, and crooks
7. Dead trees, tops, or Branches	□Dead trees □dead tops □dead branches

Table 3 Average measurements of undamaged iron-wood trees by different nondestructive techniques

Species	$D \times F$ (m Hz)	C (MPa)	D (kg/m^3)
Iron-wood trees	358.0 (106)	34.4 (9.6)	875.8 (132.4)
Norfolk island pine (Lin et al. [19])	381.3 (17.8)	25.4 (3.2)	533.4 (29.2)
Hoop pine (Lin et al. [20])	327.6 (13.2)	26.2 (3.2)	578.0 (46.2)

$D \times F$, lateral impact vibration performance; R, drilling resistance value; C, crushing strength; D, density; (), standard deviation

map grids. The decay-damaged tree had a lower average and individual stress wave velocities compared with the undamaged tree.

Some studies have reported that a stress wave or ultrasonic tomogram cannot precisely evaluate the extent and location of decay or the type of defect [7, 9, 12–14]. For example, a stress wave and ultrasonic tomogram underestimates the internal decay and overestimates that in the periphery of the trunk. Therefore, to make better assessments of internal conditions and decay of trees, other more effective methods (e.g., visual drawings of the increment core, drilling resistance and use of a fractometer) should also be adopted in combination to enhance the accuracy of the information. For example, a drilling resistance technique or increment core method can be applied to determine the position and nature of a defect for proof [1, 9, 13, 14, 22].

In-depth tree assessments are warranted when a tree poses a high degree of risk to public safety and exhibits defects that cannot be fully evaluated by visual inspection [23]. However, micro-destructive methods can destroy the compartmentalization zone and break the existing barrier zone within the tree, allowing decay to spread into healthy wood. Therefore, when using decay detection devices, the number of drill holes or sensor sites for collecting the required critical field data should be kept to a minimum [9].

A larger thickness of the peripheral region and a higher ratio of peripheral wood toward the trunk base have significant implications for the tree structure and safety (sound and health). When iron-wood trees have trunk decay, deterioration or hazardous defects, the residual wall thickness (shell) and wood quality have been found to be marginally sufficient. Most experts [3, 23–25] agree that a ratio of 30–35 % of sound wood in the remaining wall is the threshold beyond which some action should be taken.

The transversal stress wave velocity values tended to increase with increasing diameter in this study (Fig. 4). In this experiment, transversal stress wave velocity was detected by eight fixed probes along the circumference on the trunks. The properties (quality) and thickness (residual wall) of the peripheral wood in a tree is very important for the tree's structural safety and hazard evaluation. Generally, larger diameter trees with larger crowns need greater support while the trunks of smaller diameter trees with

Table 4 Transversal stress wave velocities (V) of undamaged iron-wood trees ($N = 34$)

No.	Dia. of 2D (cm)	$D \times F$ (m Hz)	V (m/s)		
			V_{max}	V_{mean}	V_{min}
1	24.2	317.9	2421	1820	1219
2	22.0	206.0	2015	1688	1361
3	36.0	451.8	2045	1687	1330
6	41.0	443.2	2109	1737	1365
7	48.6	402.7	2558	2198	1839
9	41.0	443.2	2565	2113	1662
11	60.6	360.6	3205	2571	1937
12	41.5	351.1	2614	2193	1773
14	29.5	292.1	2298	1914	1531
15	26.2	241.4	2221	1809	1398
16	37.7	324.4	2523	2140	1757
17	40.2	361.8	2656	2214	1772
18	33.1	261.0	2495	2006	1517
19	33.4	223.1	2574	2027	1481
20	31.6	230.4	2438	2022	1607
21	27.5	215.9	2231	1821	1412
22	29.3	278.6	2239	1864	1490
23	30.6	255.7	2216	1899	1583
24	25.2	216.7	2098	1791	1485
25	39.3	388.3	2510	2125	1741
27	61.1	405.1	2695	2353	2012
29	50.9	507.0	3028	2490	1952
30	48.4	457.4	2910	2190	1471
36	44.1	510.0	2888	2399	1911
38	43.5	413.3	2914	2280	1646
39	49.7	482.6	2971	2430	1890
40	40.0	384.8	2936	2226	1516
41	21.4	164.5	2028	1672	1316
42	40.7	420.4	2392	2033	1675
44	45.8	510.0	2830	2358	1886
45	54.2	558.3	3299	2635	1971
47	37.2	381.3	2765	2271	1778
48	42.3	442.9	2497	2137	1778
49	29.0	267.8	2144	1845	1547
Average	39.2 (9.5)	358.0 (105.6)	2539 (348)	2087 (265)	1636 (218)

σ_c, crushing strength; V_{min}, minimum stress wave velocity; V_{mean}, mean stress wave velocity; V_{max}, maximum stress wave velocity; (), standard deviation

smaller crowns needs to withstand smaller forces. The own (dead) weight and crown volume of the larger diameter class were larger than those of the smaller diameter class in tree. The most important and most dangerous load on the trees is undoubtedly that created by wind, which can introduce bending stresses near the periphery of the stem [26]. Previous researches has indicated that the V_{max} values of lean Norfolk island pine and lean hoop pine trees are than those of normal non-leaning trees [13, 14]. The leaning of a tree could result in reaction wood or larger gravity effects in the trunk of the tree. However, the V values of the cross section are totally influenced by the distribution of the cell structure, reaction wood, gravity, own weight, and other factors (i.e., combined action) in the tree. This might limit the application of stress wave velocity tomography. Further research is needed to clarify the intensities of individual factors in the future.

In this experiment, the $D \times F$ values generally increased with increasing stress wave velocity (V_{min}, V_{max}, and V_{mean}) values. The $D \times F$ value of lateral impact

Table 5 Transversal stress wave velocities (V) of different decay-damaged iron-wood trees ($N = 15$)

No.	Dia. of 2D (cm)	$D \times F$ (m Hz)	V (m/s)		
			V_{max}	V_{mean}	V_{min}
4	42.8	155.6	2608	1994	1380
5	31.3	156.5	2271	1639	1007
8	30.6	92.1	2102	1416	731
10	55.0	154.8	2672	1714	757
13	34.4	213.3	2401	1902	1403
26	37.2	293.9	2505	2119	1734
28	39.5	158.2	2438	1911	1385
31	48.4	452.3	2536	1995	1455
32	30.1	191.1	2458	2000	1542
33	42.8	296.2	2883	2355	1827
34	50.4	331.1	2623	2147	1671
35	45.8	395.3	2830	2337	1845
37	41.5	315.4	2438	1744	1051
43	61.6	170.6	3086	2246	1406
46	42.0	277.2	2699	2282	1865
Average	42.2 (9.1)	243.6 (102.9)	2570 (247)	1987 (274)	1404 (372)

V_{min}, minimum stress wave velocity; V_{mean}, mean stress wave velocity; V_{max}, maximum stress wave velocity; (), standard deviation

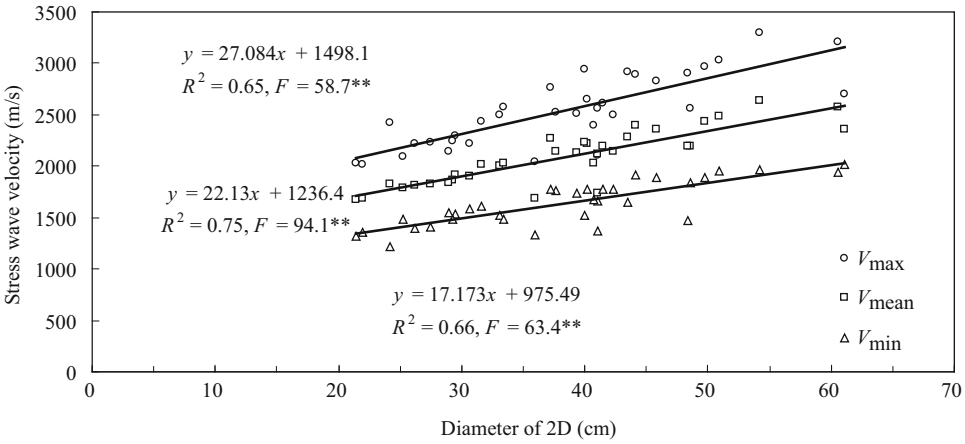

Fig. 4 Relationships between the trunk diameter and the transversal stress wave velocities of the tomogram in undamaged trees (V_{max} maximum stress wave velocity, V_{mean}, mean stress wave velocity, V_{min} minimum stress wave velocity of the tomogram)

vibration performance in living trees serves as the index of diagnosis. Moreover, the stress wave velocity tomogram of iron-wood living tree can detect the general location and area of wood deterioration. Therefore, first, this experiment suggests that the tree hazard assessment could be inspected by visual tree defects inspection. Then, general soundness or preliminary decay status could be detected by faster lateral impact vibration method. Second, the general location and area of wood deterioration could be used by transversal stress wave velocity tomography. Finally, the proposed approach can be combined with other non-destructive techniques to better examine and confirm the situations of trees.

Conclusions

A visual tree inspection form with seven categories of tree defects is proposed for tree hazard assessment in this study. The average transversal stress wave velocities were 1636–2539 m/s for undamaged iron-wood trees. Moreover, the average lateral impact vibration performance, green crushing strength, and air-dried wood density were 358.0 m Hz, 34.4 MPa, and 875.8 kg/m^3, respectively. Different nondestructive evaluated parameters could serve as the index of the diagnosis value. A table of standard values for the future use of these nondestructive methods for testing iron-wood trees with and without decay damage

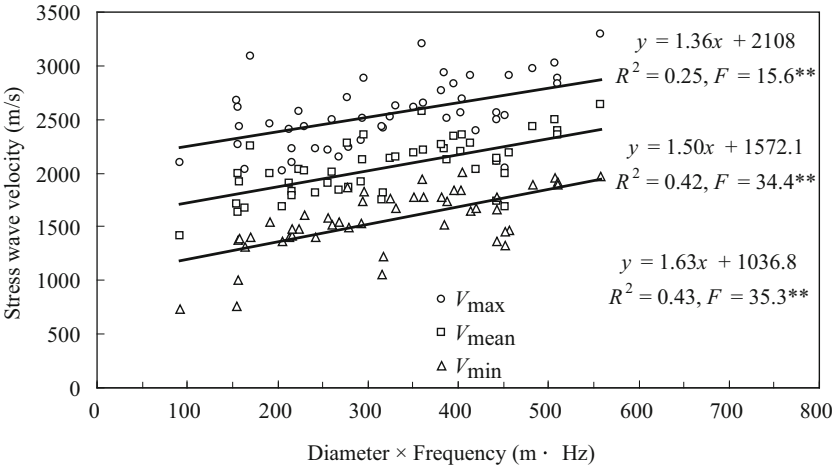

Fig. 5 Relationships between the diameter × frequency (m Hz) and the transversal stress wave velocities (m/s) of the tomogram in undamaged and damaged trees (V_{max} maximum stress wave velocity, V_{mean}, mean stress wave velocity, V_{min} minimum stress wave velocity of the tomogram)

is presented. Average $V_{\min}$ values of the trunks in decay-damaged trees were clearly lower than those of sound trees. The stress wave velocity tomogram and corresponding stress wave velocity maps of decay-damaged and undamaged iron-wood tree can detect the general location and area of wood deterioration. Moreover, general soundness or preliminary decay status could be detected by faster lateral impact vibration method. The range of demarcation between decay-damaged and undamaged wood occurred at an approximate transversal stress wave velocity of 1461–1636 m/s. The stress wave velocity ($V_{\min}$, $V_{\max}$, and V_{mean}) values increased with increasing diameter in sound trees, and the relationships could be represented by positive linear regression formulas. The $V_{\min}$ and diameter values were 1300–2000 m/s and 20–60 cm in undamaged trees, respectively. These values can be considered as the threshold values of diagnosis by stress wave velocity tomography. The proposed approach can be combined with other non-destructive techniques to better examine and confirm the situations of trees.

Acknowledgments The authors wish to thank the Experimental Forest, National Taiwan University and Taiwan Forestry Research Institute for financial support.

References

1. Wang X, Allison RB (2008) Decay detection in red oak trees using a combination of visual inspection, acoustic testing, and resistance microdrilling. Arboric Urban For 34:1–4
2. Pellerin RF, Ross RJ (2002) Nondestructive evaluation of wood. For Prod Soc, Madison, pp 150–200
3. Matheny NP, Clark JR (1994) A photographic guide to the evaluation of hazard trees in urban areas. Int Soc Arboric Champaign, IL, p 85
4. Gruber F (2008) Untenable failure criteria for trees: 1. The residual shell wall thickness rule. Arboric J 31:5–18
5. Lin CJ, Chiu CM, Wang SY (2000) Application of ultrasound in detecting wood decay in squirrel-damaged standing trees of Luanta China fir. Taiwan J For Sci 15:267–279
6. Rinn F (1999) Device for investigation materials. US-Patent US6813948; international Patent PCT/DE00/01467 (1999.05.11). (Basic patent describing sonic tomography)
7. Gilbert E, Smiley ET (2004) Picus sonic tomography for the quantification of decay in white oak (*Quercus alba*) and hickory (*Carya* spp.). Arboric J 30:277–281
8. Bucur V (2005) Ultrasonic techniques for nondestructive testing of standing trees. Ultrasonics 43:237–239
9. Wang X, Allison RB, Wang L, Ross RJ (2007) Acoustic tomography for decay detection in red oak trees. Research Paper FPL-RP-642. US Department of Agriculture, Madison
10. Deflorio G, Fink S, Schwarze FWM (2008) Detection of incipient decay in tree stems with sonic tomography after wounding and fungal inoculation. Wood Sci Technol 42:117–132
11. Lin CJ, Kao YC, Lin TT, Tsai MJ, Wang SY, Lin LD, Wang YN, Chan MH (2008) Application of an ultrasonic tomographic technique for detecting defects in standing trees. Int Biodeterior Biodegrad 43:237–239
12. Wang X, Wiedenbeck J, Liang S (2009) Acoustic tomography for decay detection in black cherry trees. Wood Fiber Sci 41:127–137
13. Lin CJ, Chang TT, Juan MY, Lin TT (2011) Detecting deterioration in royal palm (*Roystonea regia*) using ultrasonic tomographic and resistance microdrilling techniques. J Trop For Sci 23:260–270
14. Lin CJ, Chang TT, Juan MY, Lin TT, Tseng CL, Wang YN, Tsai MJ (2011) Stress wave tomography for the quantification of artificial hole detection in camphor trees (*Cinnamomum camphora*). Taiwan J For Sci 26:17–32
15. Lin CJ, Chung CH, Wu ML, Cho CL (2013) Detection of *Phellinus noxius* decay in *Sterculia foetida* tree. J Trop For Sci 25(4):487–496
16. Rinn F (2011) Basic aspects of mechanical stability of tree cross-sections. Arborist News, pp 52–54
17. Lin CJ, Wang SY, Chiu CM (2007) Crushing strength sampling with minimal damage to taiwania (*Taiwania cryptomerioides*) using a fractometer. Wood Fiber Sci 39:39–47
18. Larsson B, Bengtsson B, Gustafsson M (2004) Nondestructive detection of decay in living trees. Tree Physiol 24:853–858
19. Lin CJ, Huang YH, Huang GS, Wu ML (2015) Detection and evaluation of termite damage in Norfolk island pine (*Araucaria heterophylla*) trees by nondestructive techniques. J Exp For Nat Taiwan Univ 29:79–90

20. Lin CJ, Huang YH, Huang GS, Wu ML, Yang TH (2015) Detection of termite damage in hoop pine (*Araucaria cunninghamii*) trees by nondestructive techniques. J Trop For Sci (in press)
21. Bethge K, Mattheck C, Hunger E (1996) Equipment for detection and evaluation of incipient decay in trees. Arboric J 20:13–37
22. Wang X, Wiedenbeck J, Ross RJ, Forsman JW, Erickson JR, Pilon C, Brashaw B (2005) Nondestructive evaluation of incipient decay in hardwood logs. General Technical Report FPL-GTR-162. US Department of Agriculture, Madison
23. Pokorny JD (1992) Urban tree risk management: a community guide to program design and implementation. USDA Forest Service Northeastern Area State and Private Forestry, St. Paul
24. Harris RW, Clark JR, Matheny NP (2004) Arboriculture: integrated management of landscape trees, shrubs, and vines. Pearson Education, Upper Saddle River, pp 405–433
25. Hayes E (2007) Evaluating tree defects, a field guide. MN, Safetrees LLC, p 30
26. Mattheck C, Breloer H (1994) Field guide for visual tree assessment (VTA). Arboric J 18:1–23